

Research Article

Cite this article: Jousson A, Conedera M, Krebs P, Maspoli G, Pezzatti GB (2024) Anatomical characteristics and resprouting capacity of the underground organs of Bohemian knotweed (*Polygonum ×bohemicum*). *Weed Sci.* **72**: 172–181. doi: [10.1017/wsc.2023.77](https://doi.org/10.1017/wsc.2023.77)

Received: 28 September 2023
Revised: 7 December 2023
Accepted: 21 December 2023
First published online: 15 January 2024

Associate Editor:

Hilary A. Sandler, University of Massachusetts

Keywords:

Fallopia ×bohemica; *Reynoutria ×bohemica*; knotweeds; pith tissue; rhizome; root

Corresponding author:

Antoine Jousson;
Email: antoine.jousson@agroscope.admin.ch

© The Author(s), 2024. Published by Cambridge University Press on behalf of Weed Science Society of America. This is an Open Access article, distributed under the terms of the Creative Commons Attribution licence (<http://creativecommons.org/licenses/by/4.0/>), which permits unrestricted re-use, distribution and reproduction, provided the original article is properly cited.



Anatomical characteristics and resprouting capacity of the underground organs of Bohemian knotweed (*Polygonum ×bohemicum*)

Antoine Jousson^{1,2} , Marco Conedera³ , Patrik Krebs⁴ , Guido Maspoli⁵ and Gianni Boris Pezzatti⁴ 

¹Research Collaborator, Research Group Neobiota, Agroscope, Cadenazzo, Switzerland; ²Research Collaborator, Insubric Ecosystem Research Group, Swiss Federal Research Institute WSL, Cadenazzo, Switzerland; ³Researcher Manager, Insubric Ecosystem Research Group, Swiss Federal Research Institute WSL, Cadenazzo, Switzerland; ⁴Researcher, Insubric Ecosystem Research Group, Swiss Federal Research Institute WSL, Cadenazzo, Switzerland and ⁵Cantonal Manager, Ufficio della Natura e del Paesaggio del Canton Ticino, Dipartimento del Territorio, Bellinzona, Switzerland

Abstract

The hybrid Bohemian knotweed [*Polygonum ×bohemicum* (J. Chrtek & Chrtková) Zika & Jacobson [*cuspidatum* × *sachalinense*]; syn.: *Reynoutria ×bohemica* Chrtek & Chrtková] is part of the worldwide problematic rhizomatous invasive plants that impact (semi-)natural and agricultural systems. In this context, precise knowledge about the morpho-anatomy and resprouting capacity of the underground organs is key information for developing efficient eradication measures. In the present study, we aimed at (1) clarifying existing differences in the morpho-anatomical characteristics of rhizomes and roots, (2) developing an easy-to-apply field identification method for the underground organs, and (3) identifying the main morpho-anatomical features enhancing the rhizomes' resprouting ability. For this purpose, we collected the underground organs of two wild populations of *P. ×bohemicum* in Canton Ticino (southern Switzerland) and analyzed the morpho-anatomical differences between rhizomes and roots, using high-resolution microscope images and microtome sections. Collected material was then used for a resprouting capacity test after assessing rhizome characteristics such as weight, total diameter, pith diameter, pith brightness, and pith color. In contrast to roots, rhizomes are characterized by pith tissue in the center and display nodes with peripheral dormant buds that enable them to resprout. Resprouting ability of rhizomes was high (87.1% on average) and depended on the ontogenetic developmental stage of the organs (peak values of 97% for young and clearer-colored organs, 50% for old and dark ones). In conclusion, the smooth pith tissue of rhizomes represents a key discriminating feature between rhizomes and roots, whereas relating existing nodes to the corresponding rhizome pith color allows assessment of the resprouting potential of a knotweed population.

Introduction

Native to Japan, China, Korea, and Taiwan, the Japanese knotweeds (*Polygonum cuspidatum* Siebold & Zucc.; syn.: *Reynoutria japonica* aggr.; InfoFlora 2023) belonging to the genus *Polygonum* (syn.: *Fallopia* Adans.; syn.: *Polygonum* L.; Polygonaceae) are considered among the worst invasive neophytes in many parts of the world (Lowe et al. 2000). They are herbaceous perennial plants with annual tubular stems reaching 3- to 5-m high depending on the (sub) species (Alberternst and Böhmer 2011; InfoFlora 2023). Their dense populations can locally completely overgrow other plant species, causing major impacts on the (semi-)natural systems of concern (Aguilera et al. 2010; Gerber et al. 2010; Hejda et al. 2009; Künzi et al. 2015; Lavoie 2017; Maurel et al. 2010; Stoll et al. 2012). They reduce species richness (Aguilera et al. 2010; Stoll et al. 2012) and the abundance of soil microorganisms (Gerber et al. 2010; Stoll et al. 2012), which eventually results in a slower decomposition of the organic matter (Koutika et al. 2007; Künzi et al. 2015; Maurel et al. 2010). When invading agricultural fields, exotic *Polygonum* spp. damage infrastructures and incur additional maintenance costs due to difficulties of waste disposal (Beerling et al. 1994; Bohren 2011). Allelopathic effects on important cultivated plants have also recently been highlighted (Novak et al. 2018).

In Europe, two taxa of the *Polygonum cuspidatum* aggregate (i.e., *P. cuspidatum* Siebold & Zucc. and *P. sachalinense* F. Schmidt ex Maxim.) were imported as ornamental and fodder plants from the beginning of the 19th century (Beerling et al. 1994). Naturalization started a century later by *P. cuspidatum*, followed by *P. sachalinense* and their hybrid *Polygonum ×bohemicum* (J. Chrtek & Chrtková) Zika & Jacobson [*cuspidatum* × *sachalinense*]; syn.: *Reynoutria ×bohemica* Chrtek & Chrtková, described for the first time in 1983 in Europe



(Chrtěk and Chrtková 1983). Where both parental taxa are present, however, the hybrid form *P. ×bohemicum* eventually dominates (Bimová et al. 2003, 2004). In Switzerland, the exotic *Polygonum* spp. are found throughout all lowlands and are included in the list of invasive neophytes that identified the species proven to cause damage (InfoFlora 2023).

In the expansion process of exotic *Polygonum* spp., sexual reproduction is usually considered secondary (Conolly 1977; Locandro 1978) despite the possible important seed production by hybrid individuals (Bailey et al. 2009). The underground organs, on the contrary, are characterized by efficient and highly plastic dynamic expansion and growth, which usually start with the development of superficial woody crowns with a central taproot penetrating vertically into the ground, from which rhizomes and roots extend centrifugally (Beerling et al. 1994). Resilience characteristics of the underground organs allow these rhizomatous species to easily overcome temporary resource scarcity due to stress or disturbances (Jónsdóttir and Watson 1997; Liu et al. 2016). Vegetative resprouting capacity is characteristic of the rhizomes, whereas roots are devoid of this property (Dommanget et al. 2019). As a consequence, the expansion process is highly linked to the risks of transporting rhizome fragments through machinery, poor management of green waste, and movement of contaminated soil, as well as by natural floods that carry rhizome fragments downstream (Bohren 2011; Dawson and Holland 1999; InfoFlora 2023).

Concerning the morphological and anatomical characteristics of the underground organs, rhizomes and roots of knotweeds display a similar dark external gray-brown cortex as well as an internal tissue color that ranges from clear yellow in young organs to dark orange in older ones (Environment Agency 2013; Macfarlane 2011). As a rule of thumb, rhizomes are characterized by the presence of a large pith in the center (Fuchs 1957) as well as nodes with fine lateral roots organized in whorls. Each rhizome node displays a bud potentially able to resprout (Martin et al. 2020).

Existing literature on the resprouting capacity of rhizomes indicates a general higher resprouting potential of the hybrids with respect to parent taxa (Bimová et al. 2003; Pyšek et al. 2003) and an increasing resprouting capacity as a function of the segment length and number of nodes (Lawson et al. 2021; Sásik and Eliáš 2006). If a node is present, however, very small segments can resprout (0.2 g to 0.5 g, according to Macfarlane et al. [2011] and Lawson et al. [2021], respectively), especially in case of young organs (Environment Agency 2013). Contrary to other rhizomatic species such as common reed [*Phragmites australis* (Cav.) Trin. Ex Steud.] (Karunaratne et al. 2004; League et al. 2007) or bamboos such as *Phyllostachys* spp. (Banik 1987), no detailed information about the possible regression of the resprouting ability of rhizomes as a function of their ontogenetic development is available for knotweeds.

In this respect, the possibility of clearly distinguishing rhizomes from roots and a better understanding of the factors enhancing the rhizomes' resprouting capacity are of paramount importance for evaluating the colonization potential of a *Polygonum* population and planning targeted control measures. The overall aim of this study is to augment existing knowledge on the characteristics and reproductive capacity of the underground organs of *Polygonum ×bohemicum*, and provide the necessary information for improving possible control strategies and practical approaches against this weed. Specific aims of the study are to (1) clarify existing differences in the morpho-anatomical characteristics of rhizomes and roots, (2) develop an easy-to-apply field identification method for the

underground organs, and (3) identify the main morpho-anatomical features enhancing the rhizomes' resprouting ability. To this purpose, we collected underground organs in two wild populations of *P. ×bohemicum* in Canton Ticino (southern Switzerland), assessed the morpho-anatomical differences between rhizomes and roots, and tested the resprouting capacity of their rhizomes.

Materials and Methods

Study Area

The study area is represented by the Magadino plain, the largest alluvial plain of the Ticino River located in southern Switzerland (Figure 1). The plain is characterized by an Insubric climate, i.e., mild and dry winters and warm, but stormy summers (Klötzli 1988; Spinedi and Isotta 2004). The mean annual precipitation and the mean annual temperature are 1,806 mm and 11.9 °C, respectively (climate normal 1991 to 2020, Meteoswiss climatological station of Magadino/Cadenazzo). In Canton Ticino, the geological and soil substrate mainly consists of metamorphic crystalline rock (Labhart 1992), giving way to sandy deposits with pebbles and gravel in the floodplains, with an intermediate sandy loam soil composition at the superficial soil level (Czerski et al. 2022; Scapozza 2013). The plain is particularly rich in exotic flora and invasive neophytes (Schoenenberger et al. 2014), and among the taxa of the *P. cuspidatum* aggregate, *P. ×bohemicum* is the most widely distributed and displays the highest colonization potential.

Study Design and Workflow

As reported in Figure 2, the study was developed with two subsequent phases (i.e., Phase I in autumn 2021 and Phase II in spring 2022) and on two different sites (i.e., Gudo and Cadenazzo; see Figure 1 for location details). Both sites consist of historically important naturalized populations of *P. ×bohemicum* not subjected to control measures and currently covering more than 500 m² in an open area surrounded by cultivated fields. The hybrid *P. ×bohemicum* can reach 4.5 m height and is characterized by morphological intermediate characteristics between the two parent taxa (Alberternst and Böhmer 2011; InfoFlora 2023). The stems are partially spotted with reddish spots, and the leaves are slightly heart-shaped and can measure up to 25-cm long and 18-cm wide with trichomes situated on the veins of the abaxial side of the leaves. Preliminary field examinations using a field lens identified 0.5-mm-long trichomes (Alberternst and Böhmer 2011), which allowed us to confirm the exclusive presence of *P. ×bohemicum* at both sites.

In a first step (Phase I; Figure 2), we focused on the description of the anatomical features of the underground organs with the aim of developing a field-ready identification method to unambiguously discriminate between rhizomes and roots based on morpho-anatomical characteristics. For this purpose, at the beginning of November 2021, a 1-m-deep trench was dug with a mechanical excavator at the Gudo site. All underground organs were manually sieved from the excavated soil. Specimens of presumed rhizomes and roots were then sampled, transported to the lab facilities at the nearby research campus in Cadenazzo, cleaned of soil residuals, and processed as described in the section "Morpho-anatomical Analysis". Once the morpho-anatomical analysis of the collected specimens was concluded, a partial validation of the developed field method was made by returning to the trench dug in Gudo. The trench excavation was continued, collecting new fresh underground organs with a total diameter ranging from 0.75 to

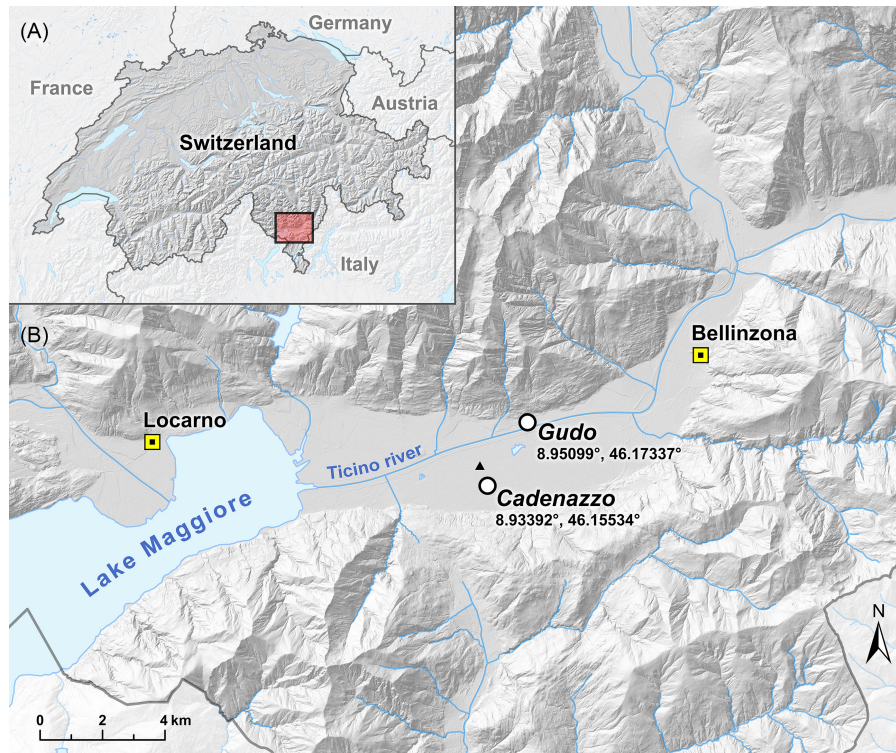


Figure 1. Study area with the location of two wild populations in Canton Ticino (Switzerland) of *Polygonum xbohemicum* (white circles), the nearby research campus (black triangle), and the two urban centers of Locarno and Bellinzona (yellow squares). (A) Map of Switzerland and (B) map of the study area (Magadino plain).

1.5 cm and preliminarily separating rhizomes and roots using the proposed protocol (pith test development in Figure 2). Based on the assumption that specimens classified as roots are not able to resprout, collected rhizomes and roots organs were first cut into 3-cm segments and subjected to a resprouting test at the greenhouse facilities of the research campus to confirm the correct distinction of rhizomes and roots (see Figure 2 and the section “Resprouting Tests”).

In a second step (Phase II; Figure 2), we focused on the morpho-anatomical features of rhizomes that increase their ability to resprout. In spring 2022 (mid-March to mid-April), we collected rhizomes ranging from 0.25 to 3 cm in total diameter from twelve 20 by 20 by 20 cm cubic soil samples excavated by hand with a shovel in Gudo and in Cadenazzo (i.e., six soil cubes at each site). Collected rhizomes were first checked for correct identification using the developed pith-test method and then cut into 3-cm segments taking care to have exactly one node in each segment. Each obtained segment was first characterized by different measurements (e.g., weight, total diameter, pith diameter, pith brightness, and pith color) and then subjected to a resprouting test at the greenhouse facilities of the research campus (see Figure 2 and the sections “Rhizome Measurements” and “Resprouting Tests”).

Morpho-anatomical Analysis

Cleaned underground organs sampled in Gudo were subjected to a preliminary visual classification into rhizomes and roots based on the external habit (Fuchs 1957; Martin et al. 2020) until ca. 25 specimens of presumed rhizomes and 25 of presumed roots were obtained. For a detailed analysis of the morpho-anatomical features, we first produced high-resolution color images depicting the external appearance and transversal sections of a selection of

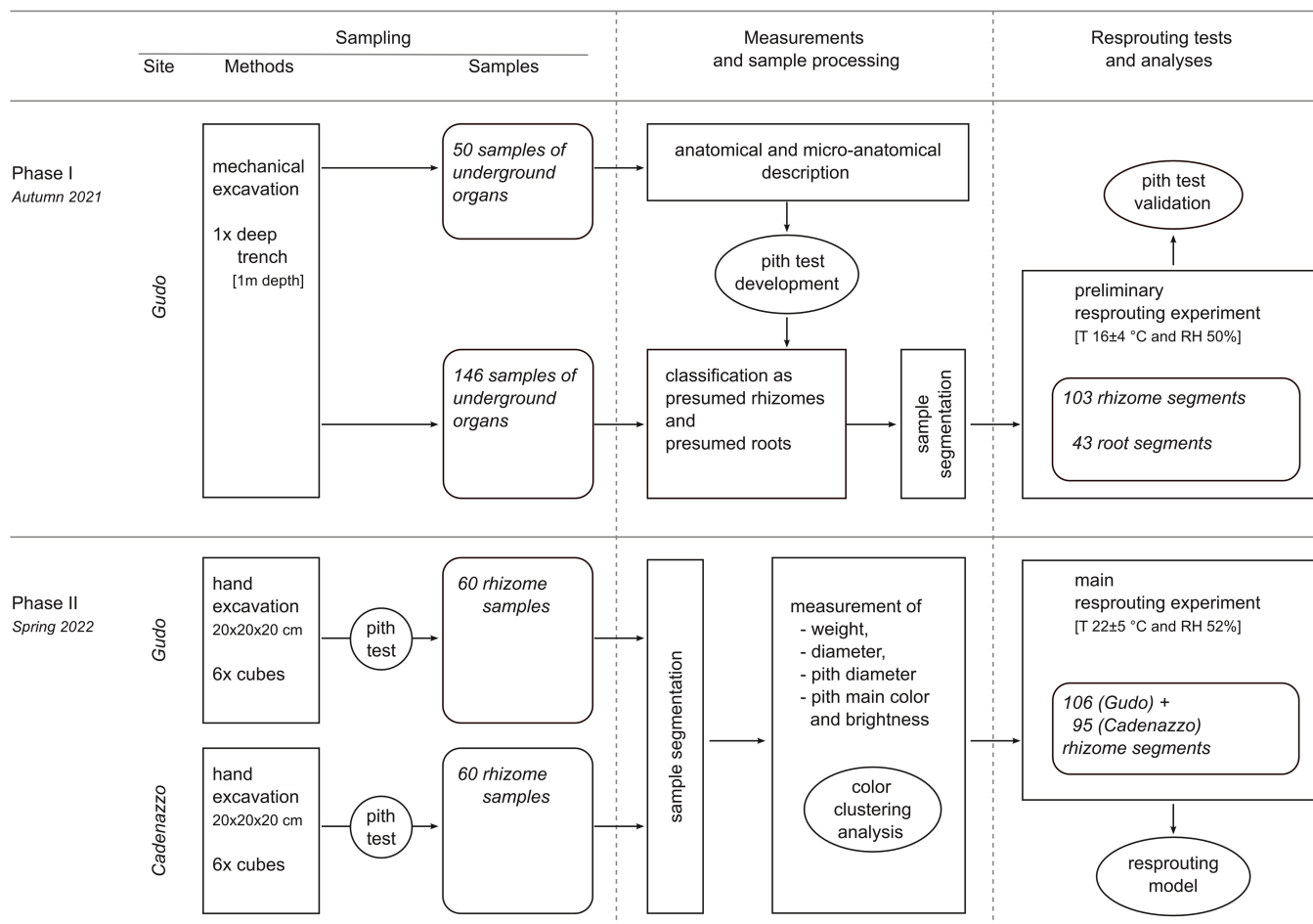
rhizomes and roots by using a stereo microscope (Olympus SZX16 with a Plan Apochromat 1× PF objective) equipped with a DP28 digital camera and stitching the obtained images with the software CellSens v. 1.16 (Olympus Corporation, 3-1 Nishi-Shinjuku 2-chome, Shinjuku-ku, Tokyo 163-0914, Japan). In the second step, samples were first put in small plastic bottles filled with 40% ethanol that was then replaced with 70% ethanol (at least four washes) for long-term conservation. Microanatomical differences between rhizomes and roots were further investigated by producing 20- μm thin slides from 10 samples of young and old rhizomes and roots. To perform thin sections, the samples were sectioned with the WSL Lab-Microtome (Swiss Federal Institute for Forest, Snow and Landscape Research, Zürcherstrasse 111, 8903 Birmensdorf, Switzerland; see also Gärtner and Schweingruber 2013). Obtained microslides were transferred onto glass slides and stained with a water solution of safranin (10 g L⁻¹) and astrablue (5 g L⁻¹) to highlight the tissues containing lignin and cellulose, respectively. Thin sections were finally fixed on slides with EUKITT mounting resins (ORSatec GmbH, Max-Fischer-Strasse 11, 86399 Bobingen, Germany) and observed under a compound upright microscope (Olympus BX53 with 5× and 10× objectives; Olympus Corporation, Tokyo 163-0914, Japan). Selected anatomical details were then photographed with the connected DP28 digital camera combined with CellSens software, and further processed with Photoshop (v. 23.5.3; Adobe Corporation, 345 Park Avenue San Jose, CA 95110-2704, USA) for cleaning or feature selection purposes.

Rhizome Measurements

Each collected 3-cm rhizome segment for the main resprouting test was subjected to different measurements (Figure 2; Table 1). We first measured the weight with a Mettler Toledo laboratory balance

Table 1. Rhizome measurements in *Polygonum xbohemicum*.

Type of variable	Variable	Unit of measure	Precision
Continuous	Weight	g	10 ⁻²
	Total diameter	mm	10 ⁻⁶
	Pith diameter	mm	10 ⁻⁶
	Pith brightness	0 to 1 (grayscale)	10 ⁻⁶
	Pith brightness classes	0 to 1 (grayscale)	10 ⁻⁶
Classes	Pith brightness classes	0 to 1 (grayscale)	10 ⁻⁶
	Pith color classes	color values (RGB)	10 ⁻⁶

**Figure 2.** Research workflow for the present study on anatomical characteristics and resprouting capacity of the underground organs of *Polygonum xbohemicum*. RH, relative humidity.

(precision at 10⁻² g; Mettler-Toledo, 1900 Polaris Parkway Columbus, OH 43240, USA). We then used the stereo microscope to take high-resolution color images with fixed parameters (magnification 0.7×, diaphragm 3.5, light source 0.9, exposure time 20 ms, and gain 3.36×) and stitched the obtained images with the CellSens software. For large diameters, the images were captured using the *Instant Multiple Image Alignment* function. On the images obtained, we measured the rhizome total diameter and pith diameter by calculating the mean between two measurements (horizontal and vertical line options of the CellSens software, precision at 10⁻⁶ mm).

To assess the rhizome pith main color, we first removed all peripheral vascular bundles and cortex from the image of each segment section using Photoshop, keeping only the pith and converting it in Tag Image File Format (.TIFF). To remove impurities and stains from the images, pith colors were clustered

for each image with R (RStudio Core Team 2023) using the *COLORDISTANCE* (Weller and Westneat 2019) and *COUNTCOLORS* (Hooper et al. 2020) packages. The clusters were built on all pith pixels, and the frequencies of the five most frequent RGB clusters were calculated using *getKMeanColors* and *extractClusters* functions in *COLORDISTANCE* package (Weller and Westneat 2019). Finally, only the first or two most frequent color clusters (at least 20% frequency) were retained and, if applicable, averaged.

From the obtained pith main RGB colors, we calculated the corresponding pith brightness along a continuous grayscale ranging from 0 (black) to 1 (white) using the *rgb2gray.luminosity* function of the *PLOTTER* package (Weise 2019). To enhance visualization and define ordered color scales that are simple and easy to use in the field, we calculated six pith brightness classes and six color classes. Brightness classes were obtained by dividing the value range into six regular intervals. RGB color values were also

Table 2. Estimate statistics of the fitted generalized linear mixed model for resprouting ability (logistic) in *Polygonum xboheicum* ($n_{\text{tot}} = 201$).

Variable ^a	Estimate	CI 2.5%	CI 97.5%	P-value	vif
(Intercept)	-2.92	-5.34	-0.66	0.01	—
Pith brightness ^b	6.81	3.89	10.08	< 0.01	1.24
Total diameter	1.15	-0.43	3.28	0.21	1.87
Pith diameter	0.43	-4.01	4.98	0.85	1.58

^aWeight was removed to avoid multicollinearity with total diameter.

^bPith brightness corresponding to the continuous grayscale (0–1).

clustered into six color classes by using the *kmeans* function on the RGB values matrix.

Resprouting Tests

The resprouting tests took place in the greenhouse facilities of the research campus in Cadenazzo. For this purpose, the 3-cm segments of the underground organs were buried 1.5-cm deep in a 5-cm-deep mixture of sand and loam (soil composition: 1 part silt loam, 1 part sand, 1 part manure, and 1 part expanded shale) in plastic trays (Cindy Seed trays with sieve bottom; Caminada Sementi SA, Via Pré d'La, 6814 Lamone, Switzerland), into which water was added daily to maintain soil moisture. In both preliminary and main resprouting experiments (see Figure 2), trays were inspected for resprouting specimens every 2 to 3 d for a total experimental period of 70 d. The preliminary resprouting test took place late November 2021 with 103 rhizome and 43 root segments which were kept at a mean temperature of 16 ± 4 C and at 50% relative air humidity. The main resprouting test took place in April 2022 with 201 rhizome segments in total (106 from Gudo and 95 from Cadenazzo), which were kept at 22 ± 5 C with 52% relative air humidity.

Statistical Analysis

To identify the features enhancing the rhizomes' resprouting ability, we tested whether relationships between the continuous variables and resprouting capacity encoded as a binary response were significant. The *glmer* function in LME4 package (Bates et al. 2015) was used to perform a binomial model (fitting generalized linear models, binomial multivariate), assessing all morphological rhizome patterns. A mixed-modeling approach was applied, as we were not interested in the effect provided by the site (random factor). To avoid multicollinearity, the variance inflation factor (*vif*) was calculated, and the model was adapted. We then calculated the model *R squared* using the MUMLN package (Bartoń 2023), as well as the estimates of the retained variables, their confidence intervals (2.5% and 97.5%), their P-values in the model, and their respective *vif* values (Table 2).

To assess the informative and diagnostic value of pith chromatic characteristics, curves representing the resprouting capacity for all pith brightness and color classes were calculated. Differences in resprouting capacity among classes were tested using Pearson's chi-square tests (Hope 1968). To provide easily usable color scales to assess rhizome resprouting capacity in the field, we analyzed the differences among pith color classes (Supplementary Figure S1). Differences in pith brightness values (i.e., continuous grayscale) were visualized as box plots among pith color classes. Significant mean differences were tested with Kruskal-Wallis for general mean comparison and Wilcoxon tests

for pairwise comparisons (Hollander and Wolfe 1973) using a false discovery rate correction (Benjamini and Yekutieli 2001). Significant nominal levels of 1% and 5% were used for general and pairwise comparisons, respectively. In addition, a practical fact sheet with reference color scales representing the pith brightness and color classes was developed (Supplementary Figure S2). All analyses were performed in R (RStudio Core Team 2023).

Results and Discussion

Morpho-anatomy of the Underground Organs

The external appearance of the epidermis of underground organs looked quite similar in texture and color for both rhizomes and roots (Figure 3). It appeared clear brown in young rhizomes (Figure 3A) and young roots (Figure 3E) and became darker with aging and thickening (Figure 3C and 3G for rhizomes and roots, respectively). A distinctive (although not always unambiguous) external feature on the extensively (stolon-like) elongate rhizomes was represented by the presence of nodes provided of small lateral roots organized in whorls and a rudimentary and scale-like bud at regular internodal intervals (Figure 3A and 3C). Roots, however, did not display nodes and had small, single lateral root hairs irregularly distributed along and around the organ (Figure 3E and 3G).

Anatomical analyses of the cross sections provided additional clear distinctive features between rhizomes and roots, consisting of a central soft pith tissue characterizing the rhizomes (Figure 3B and 3D) but absent in roots (Figure 3F and 3H). The pith size of the rhizomes remained constant and measured approximately 4 to 5 mm, whereas the pith tissue turned from clear to dark colors (orange to brown-purple) with the aging of the rhizome (Figure 3B and 3D). As a result, the pith to section ratio was higher in young rhizomes with respect to older and thicker ones.

The micro-anatomical structure of the juvenile rhizomes (Figure 4A) revealed the presence of single xylem vascular bundles in formation surrounding a large central pith. Outside the cambium, there was phloem tissue in formation surrounded by a clear pericyclic circle, a cortex, a thin phellem tissue, and an external epidermis. In mature rhizomes (Figure 4C), the pith was surrounded by single vascular bundles of xylem, a ring of phloem bundles, a cortex, and a thin phellem. When rhizomes became thicker, part of the phloem collapsed. Xylem lignification was an irregular ontogenetic process that started along rays. Figure 4E shows the detailed structure of a node cross section with the bud originating from the main pith and characterized by a large meristematic zone (corpus and tunica) protected by a multitude of scale leaves also known as cataphylls (Figure 4C).

In contrast to rhizomes, roots displayed a central part of homogeneous ligneous consistency composed of xylem bundles and vessels organized along the rays (Figure 4B and 4D). The external part of the root consisted of phloem tissue followed by a cortex, a thin phellem tissue, and an external epidermis. Single lateral root hairs originated from the center (Figure 4F).

Finally, druses containing calcium oxalate crystals represented a common feature of rhizomes and roots (Figure 4A–D) and were present irrespective of ontogenetic stage. Oxalate crystals have been already reported for other invasive *Polygonum* taxa (Fuchs 1957; Khalil et al. 2020) and are considered important plant defense factors against herbivory and tissue degradation (Nakata 2003; Prasad and Shivay 2017).

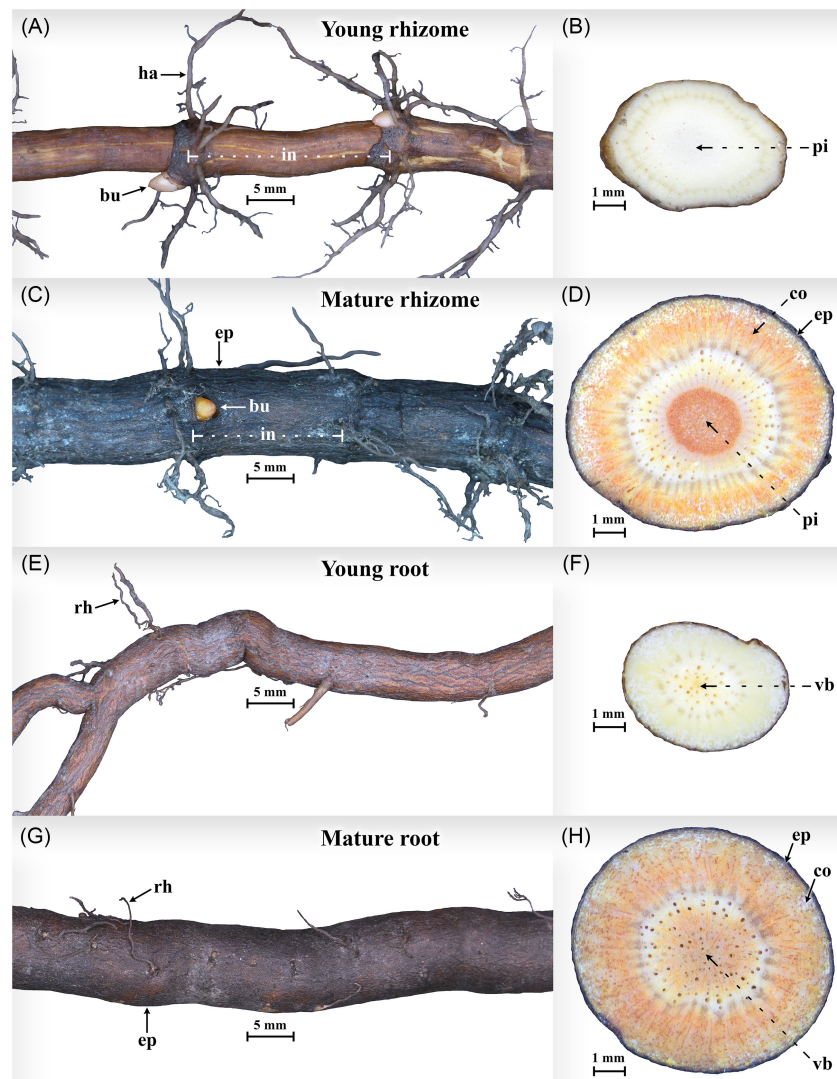


Figure 3. Morphology of rhizomes and roots of *Polygonum xbohemicum*. (A and B) Young rhizome; (C and D) mature rhizome; (E and F) young root; (G and H) mature root. bu, rhizome bud; co, cortex; ep, epidermis; ha, rhizome hair; in, internodal interval; pi, pith; rh, root hair; vb, vascular bundles.

Discriminating between Rhizomes and Roots

Based on the differences in key anatomical features of cross sections such as the soft pith tissue in the rhizomes, we propose a three-step method to discriminate between rhizomes and roots to be applied in succession if no unambiguous conclusion is reached. As a first step, we look at the presence of nodes provided of whorls of lateral roots and a single bud (rhizomes) or just small, single lateral root hairs irregularly distributed along and around the organ (roots). If this criterion does not allow for a conclusive discrimination between the two organs, we suggest proceeding with the pith-test. The pith-test consists of inserting a pointed and hard object (needle, pocketknife, pencil) into the central part of the concerned underground organ to test the compactness of the tissue. The central pith tissue is soft and easy to penetrate, whereas roots possess a harder and uniformly woody texture, which makes penetrating it very hard (see also: <https://youtu.be/3V8eHq5K5bA>). In case of remaining doubts, one can further check for the presence of the pith tissue, which is characteristic of rhizomes, by means of a folding pocket magnifier or a field lens.

Resprouting Tests

In the preliminary resprouting test, all 43 segments classified as root after the pith-test verification failed to resprout (0/43: 0%). Presumed rhizome segments, on the contrary, displayed an overall resprouting rate of 88.3% (i.e., 91/103).

In the main resprouting test, rhizome segments displayed an overall resprouting rate of 87.1% (i.e., 175/201). Concerning the pith brightness classes, we found 21 rhizome segments representative of class 0.84–0.96, 51 of class 0.72–0.84, 42 of class 0.60–0.72, 34 of class 0.48–0.60, 32 of class 0.36–0.48, and 21 of class 0.24–0.36; whereas for the pith color classes, 35 segments were representative of class #E1D9D4, 51 of #CEBCB0, 45 of #B59A90, 22 of #9C7A78, 28 of #80606E, and 20 of #624A62. The comparison between the pith color classes and the pith brightness (i.e., continuous grayscale) revealed that all classes have significantly different means of pith brightness values (P -value < 0.01 for general mean comparison and all P -values < 0.05 for all pairwise comparisons; Supplementary Figure S1).

Regarding the mixed-modeling approach, the rhizome total diameter was strongly correlated with rhizome biomass, as the *vi*f

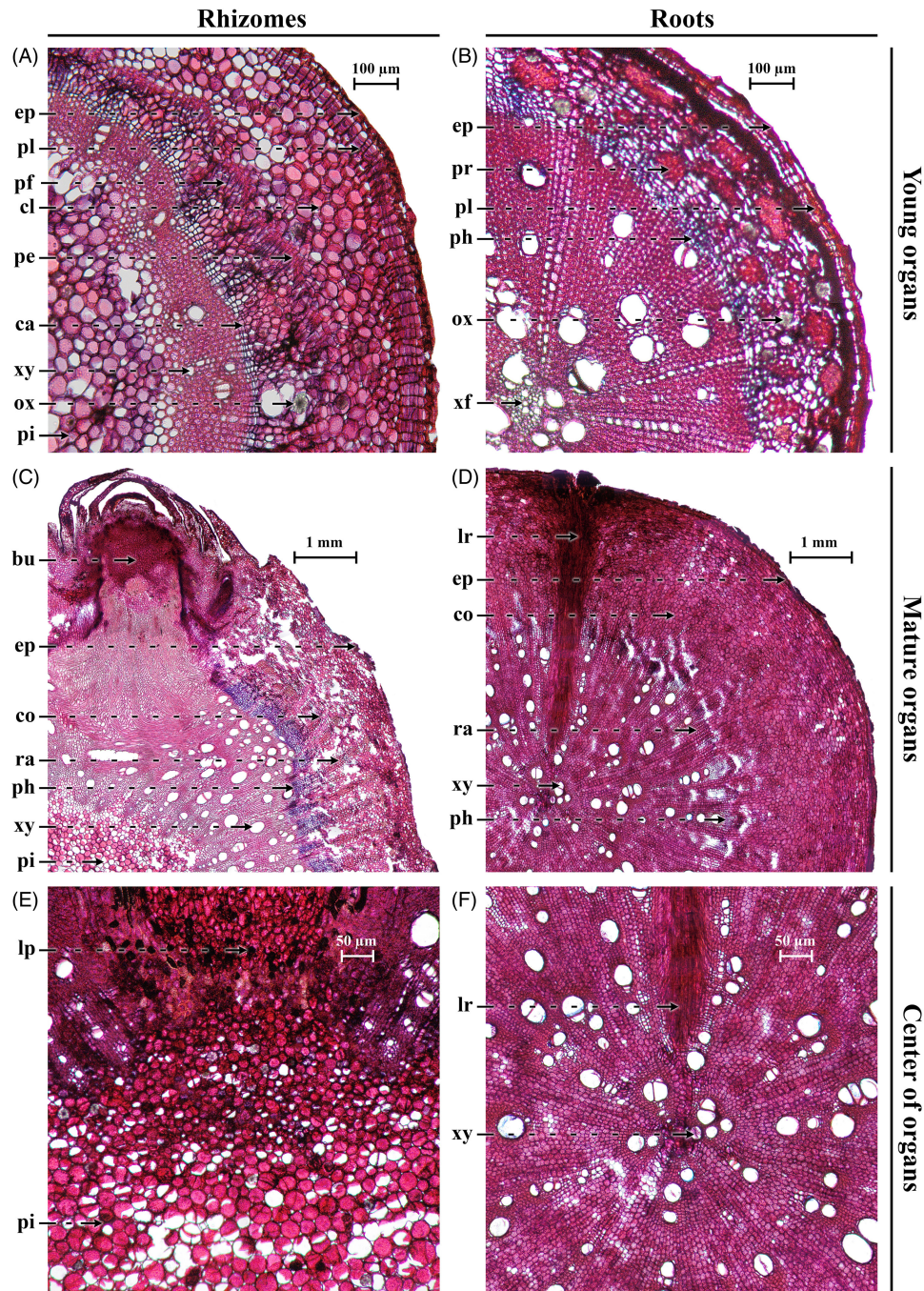


Figure 4. Anatomy of rhizomes and roots of *Polygonum xbohemicum*. (A) Young rhizome; (B) young root; (C) mature rhizome; (D) mature root; (E) mature rhizome center; (F) mature root center. bu, rhizome bud; ca, cambium; cl, collenchyma; co, cortex; ep, epidermis; lp, lateral pith; lr, lateral root; ox, calcium oxalate; pe, pericycle; pf, phloem in formation; ph, phloem; pi, pith; pl, phellem; pr, pericyclic fibers; ra, ligneous ray; xf, xylem in formation; xy, xylem.

values were higher than 5 (10.14 and 7.04, respectively). To avoid multicollinearity in the model, only the total diameter was therefore retained, as it represents the easier variable directly measurable in the field. The generalized linear model returned an R^2 of 26.8% (delta equal to 12.1%), with only the pith brightness variable significantly contributing to the best fit of the model (P-value < 0.01 with confidence intervals that do not overlap 0; see Table 2).

The resprouting rate reached 95% and 97% for the clearest pith brightness class 0.84–0.96 and color class (#E1D9D4), respectively,

whereas the darkest pith brightness class 0.24–0.36 and color class (#624A62) displayed resprouting rates of 52% and 50%, respectively (Figure 5). Differences in resprouting capacities were significant among pith brightness classes ($\chi^2 = 29.4$, $df = 5$, P-value < 0.01), as well as among pith color classes ($\chi^2 = 31.1$, $df = 5$, P-value < 0.01). The comparison between the two pith color scales indicated that the three clearest classes of pith brightness displayed very similar resprouting rates ranging from 94% to 95% (Figure 5A), whereas the three clearest pith color classes displayed resprouting rates ranging from 91% to 97% (Figure 5B), meaning

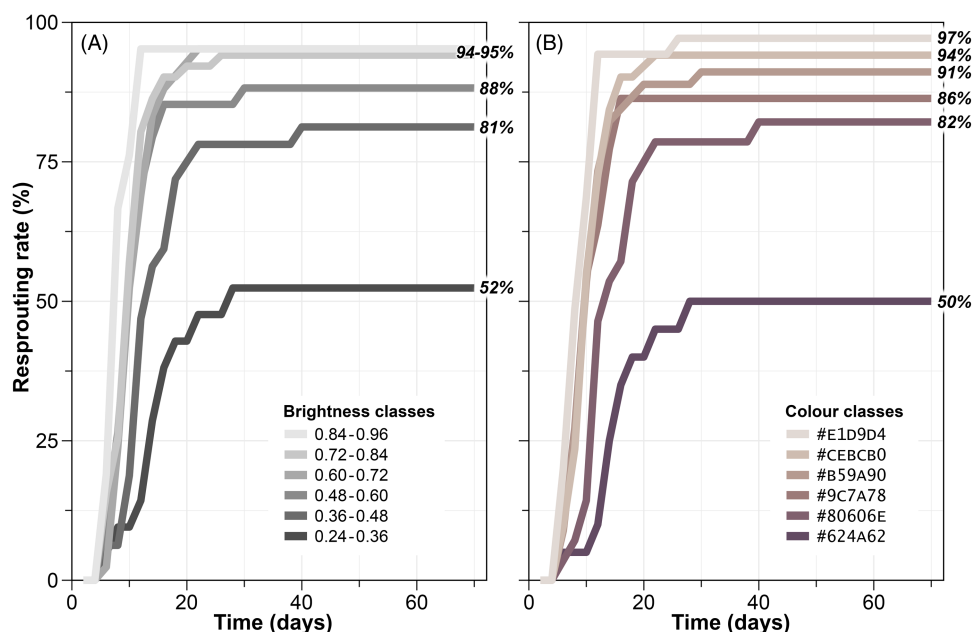


Figure 5. Resprouting rate for each pith color class (time days = 70; $n_{\text{tot}} = 201$) in *Polygonum xbohemicum*. (A) using the six pith brightness classes according to grayscale [0–1] intervals and (B) using the six color classes for which the reference RGB color is indicated in Hex Code. Differences in resprouting capacities (resprouting rates) were significant among pith brightness classes ($\chi^2 = 29.4$, $df = 5$, P -value < 0.01), as well as among pith color classes ($\chi^2 = 31.1$, $df = 5$, P -value < 0.01).

that color classes were more precise for discriminating rhizome resprouting capacities for the clearest pith sections.

Previous studies on the resprouting capacity of *Polygonum* rhizomes already highlighted the high response capacity of *Polygonum* taxa in this respect, even in case of very small segments, as long as they are provided by a bud (Lawson et al. 2021; Macfarlane 2011; Martin et al. 2020). Existing literature additionally reports a better vegetative resprouting capacity of longer rhizome segments (Sásik and Eliáš 2006), of the hybrid genotypes (Bímová et al. 2003; Pyšek et al. 2003), as well as greater resprouting success in cases of overall higher density of nodes and related buds in the soil (Lawson et al. 2021).

Our results concerning the overall resprouting rates of *Polygonum xbohemicum* (i.e., 87.1%) are in line with the rate of 85% reported by Weber (2011) for the highly invasive giant goldenrod (*Solidago gigantea* Alton) and is markedly higher with respect to the rate of 50.9% reported by League et al. (2007) for clear rhizomes of *P. australis*. Here, we further demonstrated that as highlighted for *P. australis* (e.g., Karunaratne et al. 2004; League et al. 2007), the resprouting capacity of *P. xbohemicum* rhizomes is highly dependent on the ontogenetic stage of the organ, which in turn is reflected by the color of the pith tissue. In short, the younger and clearer the pith, the higher the probability of a successful resprouting; the darker the pith color, the lower the resprouting capacity of the rhizome. This partially contrasts with what is reported for *S. gigantea* (Weber 2011) and *Calligonum arborescens* Litv. (Luo and Zhao 2015), which tend to display higher regeneration rates for larger organs. To practically implement this result for knotweeds, we propose two field-ready reference scales, one as grayscale for pith brightness (applicable also in case of decreased ability to distinguish colors) and the other as ordered color classes (Supplementary Figure S2).

Finally, *Polygonum* populations do not display resprouting capacities of underground organs other than rhizomes unlike other very invasive species, that may spread via stolons or rhizomatous

roots (Clarke et al. 2012; Cornelissen et al. 2014; Song et al. 2012). With regard to management strategies, it is fundamental to first distinguish between rhizomes and roots, as the roots do not possess any resprouting capacity (Dommanget et al. 2019). In addition, pith color allows new perspectives in the assessment of rhizome vitality and resprouting potential of a *Polygonum* population. It represents an important variable to be considered for planning resprouting tests or for assessing the rhizomes' resprouting capacity in the field. The results of this study and the suggested practical approaches may represent an important step forward in optimizing the management and control strategies of rhizomatous invasive species such as knotweeds. Focusing on the presence and quality of the rhizomes to define the necessary treatments can significantly reduce workload and related financial and human resources.

Supplementary material. To view supplementary material for this article, please visit <https://doi.org/10.1017/wsc.2023.77>

Acknowledgments. For financial support, we would like to thank the Section of the Territorial Development (Office of Nature and Landscape), the Section for the Protection of Air, Water and Soil (Office of Waste and Contaminated Sites) of Canton Ticino and the Gruppo di Lavoro Organismi Alloctoni Invasivi in Canton Ticino (GLOAI). For their collaboration during all phases of the project, we would like to thank Mauro Togni (Canton Ticino and GLOAI) and Gisella Novi (Canton Ticino and GLOAI). For the fieldwork, we would like to thank Gottardo Pestalozzi (WSL Birmensdorf), Samuele Peduzzi (Agroscope Cadenazzo), and all field helpers during the excavations. The authors declare no competing interests.

References

- Aguilera AG, Alpert P, Dukes JS, Harrington R (2010) Impacts of the invasive plant *Fallopia japonica* (Houtt.) on plant communities and ecosystem processes. *Biol Invasions* 12:1243–1252
- Alberterst B, Böhmer HJ (2011) NOBANIS—Invasive Alien Species Fact Sheet: *Fallopia japonica*. Online Database of the European Network on

- Invasive Alien Species. https://www.nobanis.org/globalassets/speciesinfo/r/reynoutria-japonica/reynoutria_japonica4.pdf. Accessed: September 6, 2023
- Bailey JP, Bímová K, Mandák B (2009) Asexual spread versus sexual reproduction and evolution in Japanese knotweed s.l. sets the stage for the “battle of the clones.” *Biol Invasions* 11:1189–1203
- Banik RL (1987) Techniques of bamboo propagation with special reference to prerooted and prerhizomed branch cuttings and tissue culture. Pages 160–169 in Rao AN, Dhanarajan G, Sastry CB, eds. *Recent Research on Bamboos*. Beijing: Chinese Academy of Forestry. 393 p
- Bartoň K (2023) MuMIn: Multi-Model Inference, R Package Version 1.47.5. <https://cran.r-project.org/web/packages/MuMIn/MuMIn.pdf>. Accessed: September 6, 2023
- Bates D, Mächler M, Bolker B, Walker S (2015) Fitting linear mixed-effects models using lme4. *J Stat Softw* 67:1–48
- Beerling DJ, Bailey JP, Conolly AP (1994) Biological flora of the British Isles. *Fallopia japonica* (Houtt.) Ronse Decraene. *J Ecol* 82:959–979
- Benjamini Y, Yekutieli D (2001) The control of the false discovery rate in multiple testing under dependency. *Ann Stat* 29:1165–1188
- Bímová K, Mandák B, Kašparová I (2004) How does *Reynoutria* invasion fit the various theories of invasibility? *J Veg Sci* 15:495–504
- Bímová K, Mandák B, Pyšek P (2003) Experimental study of vegetative regeneration in four invasive *Reynoutria* taxa (Polygonaceae). *Plant Ecol* 166:1–11
- Bohren C (2011) Exotic weed contamination in Swiss agriculture and the non-agriculture environment. *Agron Sustain Dev* 31:319–327
- Chrtěk J, Chrtěková A (1983) *Reynoutria* × *bohemica*, nový kříženeček z čeledi rdesnovitých. *Čas Nár Muz Praze Rada Přír* 152:120
- Clarke PJ, Lawes MJ, Midgley JJ, Lamont BB, Ojeda F, Burrows GE, Enright NJ, Knox KJE (2012) Resprouting as a key functional trait: how buds, protection and resources drive persistence after fire. *New Phytol* 197:19–35
- Conolly AP (1977) The distribution and history in the British Isles of some alien species of *Polygonum* and *Reynoutria*. *Watsonia* 11:291–311
- Cornelissen JHC, Song YB, Yu FH, Dong M (2014) Plant traits and ecosystem effects of clonality: a new research agenda. *Ann Bot* 114:369–376
- Czerski D, Giacomazzi D, Scapozza C (2022) Evolution of fluvial environments and history of human settlements on the Ticino river alluvial plain. *Geogr Helv* 77:1–20
- Dawson FH, Holland D (1999) The distribution in bankside habitats of three alien invasive plants in the U.K. in relation to the development of control strategies. *Hydrobiologia* 415:193–201
- Dommanget F, Evette A, Martin FM, Piola F, Thiébaud M et al. (2019) Les renouées asiatiques, espèces exotiques envahissantes. *Sciences Eaux & Territoires* 27:8–13
- Environment Agency (2013) *Managing Japanese Knotweed on Development Sites: The Knotweed Code of Practice*. Bristol, UK: Environment Agency Publications. 72 p
- Fuchs C (1957) Sur le développement des structures de l'appareil souterrain du *Polygonum cuspidatum* Sieb. et Zucc. *Bull Soc Bot Fr* 104:141–147
- Gärtner H, Schweingruber F (2013) *Microscopic Preparation Techniques for Plant Stem Analysis*. Remagen-Oberwinter, Germany: Verlag Dr. Kessel. 78 p
- Gerber E, Murrell C, Krebs C, Bilat J, Schaffner U (2010) *Evaluating Non-chemical Management Methods against Invasive Exotic Knotweeds, Fallopia spp.* Final Report. Egham, UK: CABI International. 24 p
- Hejda M, Pyšek P, Jarošík V (2009) Impact of invasive plants on the species richness, diversity and composition of invaded communities. *J Ecol* 97:393–403
- Hollander M, Wolfe DA (1973), *Nonparametric Statistical Methods*. New York: Wiley. 120 p
- Hooper SE, Weller H, Amelon SK (2020) CountColors, an R package for quantification of the fluorescence emitted by *Pseudogymnoascus destructans* lesions on the wing membranes of hibernating bats. *J Wildl Dis* 56:759–767
- Hope ACA (1968) A simplified Monte Carlo significance test procedure. *J R Stat Soc* 30:582–598
- InfoFlora Database (2023) *Reynoutria japonica* aggr. <https://www.infoflora.ch/de/flora/reynoutria-japonica-aggr.html>. Accessed: September 6, 2023
- Jónsdóttir I, Watson M (1997) Extensive physiological integration: an adaptive trait in resource-poor environments. Pages 109–136 in de Kroon H, van Groenendael J, eds. *The Ecology and Evolution of Clonal Plants*. Leiden: Backhuys
- Karunaratne S, Asaeda T, Toyooka S (2004) Colour-based estimation of rhizome age in *Phragmites australis*. *Wet Ecol Manag* 12:353–363
- Khalil AAK, Akter KM, Kim HJ, Park WS, Kang DM, Koo KA, Ahn MJ (2020) Comparative inner morphological and chemical studies on *Reynoutria* species in Korea. *Plants* 9:222
- Klötzli F (1988) On the global position of the evergreen broad-leaved (non-ombrophilous) forest in the subtropical and temperate zone. *Veröf Geobot Inst ETH Zürich* 98:169–196
- Koutika LS, Vanderhoeven S, Chapuis-Lardy L, Dassonville N, Meerts P (2007) Assessment of changes in soil organic matter following invasion by exotic plant species. *Biol Fertil Soils* 44:331–341
- Künzi Y, Prati D, Fischer M, Boch S (2015) Reduction of native diversity by invasive plants depends on habitat conditions. *Am J Plant Sci* 6:2718–2733
- Labhart TP (1992) *Geologie der Schweiz*. Berlin: Medimops. 211 p
- Lavoie C (2017) The impact of invasive knotweed species (*Reynoutria* spp.) on the environment: review and research perspectives. *Biol Invasions* 19:2319–2337
- Lawson JW, Fennell M, Smith MW, Bacon KL (2021) Regeneration and growth in crowns and rhizome fragments of Japanese knotweed (*Reynoutria japonica*) and desiccation as a potential control strategy. *PeerJ* 9:e11783
- League MT, Seliskar DM, Gallagher JL (2007) Predicting the effectiveness of *Phragmites* eradication measures using a rhizome growth potential bioassay. *Wet Ecol Manag* 15:27–41
- Liu F, Liu J, Dong M (2016) Ecological consequences of clonal integration in plants. *Front Plant Sci* 7:770–781
- Locandro RR (1978) Weed watch. Japanese bamboo. *Weeds Today* 9:21–22
- Lowe S, Browne M, Boudjelas S, De Poorter M (2000) 100 of the World's Worst Invasive Alien Species: A Selection from the Global Invasive Species Database. Auckland: Invasive Species Specialist Group, Species Survival Commission of the IUCN. 12 p
- Luo W, Zhao W (2015) Burial depth and diameter of the rhizome fragments affect the regenerative capacity of a clonal shrub. *Ecol Complex* 23:34–40
- Macfarlane J (2011) *Development of Strategies for the Control and Eradication of Japanese Knotweed*. Ph.D dissertation. Exeter, Devon, UK: University of Exeter. 330 p
- Martin FM, Dommanget F, Lavallée F, Evette A (2020) Clonal growth strategies of *Reynoutria japonica* in response to light, shade, and mowing, and perspectives for management. *NeoBiota* 56:89–110
- Maurel N, Salmon S, Ponge JF, Machon N, Moret J, Muratet A (2010) Does the invasive species *Reynoutria japonica* have an impact on soil and flora in urban wastelands? *Biol. Invasions* 12:1709–1719
- Nakata PA (2003) Advances in our understanding of calcium oxalate crystal formation and function in plants. *Plant Sci* 164:901–909
- Novak N, Novak M, Barić K, Šćepanović M, Ivić D (2018) Allelopathic potential of segetal and ruderal invasive alien plants. *J Cent Eur Agric* 19:408–422
- Prasad R, Shivay YS (2017) Oxalic acid/oxalates in plants: from self-defence to phytoremediation. *Curr Sci* 112:1665–1667
- Pyšek P, Brock JH, Bímová K, Mandák B, Jarošík V, Koukolíková I, Pergl J, Štěpánek J (2003) Vegetative regeneration in invasive *Reynoutria* (Polygonaceae) taxa: the determinant of invasibility at the genotype level. *Am J Bot* 90:1487–1495
- RStudio Core Team (2023) RStudio: Integrated Development for R. Boston: RStudio, PBC. <http://www.rstudio.com>. Accessed: September 6, 2023
- Sásik R, Eliáš P (2006) Rhizome regeneration of *Fallopia japonica* (Japanese knotweed) (Houtt.) Ronse Decr. I. Regeneration rate and size of regenerated plants. *Folia Oecol* 33:57–63
- Scapozza C (2013) L'evoluzione degli ambienti fluviali del Piano di Magadino dall'anno 1000 a oggi. *Arch Storico Ticin* 153:60–92
- Schoenenberger N, Rötliberger J, Carraro G (2014) La flora esotica nel Cantone Ticino. *Boll Soc Ticin Sci Nat* 102:13–30
- Song YB, Yu FH, Li JM, Keser LH, Fischer M, Dong M, van Kleunen M (2012) Plant invasiveness is not linked to the capacity of regeneration from small fragments: an experimental test with 39 stoloniferous species. *Biol Invasions* 15:1367–1376
- Spinedi F, Isotta F (2004) Il clima del Ticino. *Dati, statistiche e società* 6:4–39

- Stoll P, Gatzsch K, Rusterholz HP, Baur B (2012) Response of plant and gastropod species to knotweed invasion. *Basic Appl Ecol* 13:232–240
- Weber E (2011) Strong regeneration ability from rhizome fragments in two invasive clonal plants (*Solidago canadensis* and *S. gigantea*). *Biol Invasions* 13:2947–2955
- Weise T (2019) An R Package with Utilities for Graphics and Plots. <https://github.com/thomasWeise/plotteR#readme>. Accessed: September 6, 2023
- Weller H, Westneat M (2019) Quantitative color profiling of digital images with earth mover's distance using the R package colordistance. *PeerJ* 7: e6398